On the detectivity of quantum-dot infrared photodetectors

V. Ryzhii[a] and I. Khmyrova
Computer Solid State Physics Laboratory, University of Aizu, Aizu-Wakamatsu 965-8580, Japan

V. Mitin
Department of Electrical and Computer Engineering, Wayne State University, Detroit, Michigan 48202

M. Stroscio
US Army Research Office, P.O. Box 12211, Research Triangle Park, North Carolina 27709

M. Willander
Department of Microelectronics and Nanoscience, Chalmers University of Technology and Gothenburg University, Gothenburg S-412 96, Sweden

(Received 31 January 2001; accepted for publication 28 March 2001)

We report on the analysis of thermally-limited operation of quantum-dot infrared photodetectors (QDIPs). A device model is developed and used to calculate the QDIP detectivity as a function of the structural parameters, temperature, and applied voltage, as well as to determine the conditions for the detectivity maximum. The QDIP detectivity is compared with that of quantum-well infrared photodetectors (QWIPs). This work clarifies why the existing QDIPs are still inferior to QWIPs and shows that a significant improvement in the QDIP performance can be accomplished by the utilization of dense QD arrays with small QDs. © *2001 American Institute of Physics.*
[DOI: 10.1063/1.1376435]

As predicted theoretically,[1] quantum-dot infrared photodetectors (QDIPs) can surpass quantum well infrared photodetectors (QWIPs). A number of research groups have reported fabrication and experimental studies of InAs/GaAs, InGaAs/GaAs, InGaAs/InGaP, and Ge/Si QDIPs.[2–15] Most of fabricated and measured QDIPs exhibited performance inferior to that of QWIPs. One may suppose that the structural parameters of existing QDIP samples are far short of optimum. As QDIPs have many potential applications, their optimization makes sense only once the details of the application are specified. For example, such an optimization can be different in the case of QDIPs displaying a background limited infrared performance and in the thermal limit. In this letter, we analyze the features of QDIP characteristics and discuss the problem of the optimization of QDIPs using a recently developed physical model.[16,17] In the framework of this model, we calculate the QDIP thermally limited detectivity as a function of the structural parameters, temperature, and applied voltage and consider the conditions for its maximum.

The QDIP under consideration consists of a stack of QD (InAs or InGaAs) arrays (layers) separated by wide-gap material layers (for example, GaAs). Each QD array includes periodically distributed identical QDs. The QD arrays are doped with donors. Such a structure, which plays a role of the QDIP active region, is sandwiched between two heavily doped regions made of the same material as that in which QDs are buried. These regions serve as the emitter and collector contacts. We focus on QDIPs with multiple QD arrays of large-size QDs. Each QD has a large number of bound states and, therefore, is capable of accepting many electrons. A schematic view of the QDIP structure under consideration is shown in Fig. 1.

Both in dark conditions and under illumination, the current across the QDIP in question at the applied voltage is accompanied by the following processes: Thermo- and photoexcitation of electrons from bound states in QDs into continuum states, capture of mobile electrons into QDs (transitions from continuum into bound states), transport of mobile electrons between the potential ''hills'' formed by charged QDs, injection of extra electrons from the emitter contact because of the redistribution of the potential in the QDIP active region caused by the change in the charges accumulated by QDs, and collection of the excited and injected electrons by the pertinent contact. The main features of QDIPs (which differentiate them from QWIPs) are associated with the discreteness of the QD energy spectrum leading to a dependence of the thermoactivation energy on the QD sizes, strong sensitivity to normally incident radiation, phonon bottleneck effect (or similar effects[18–20]) in the electron cap-

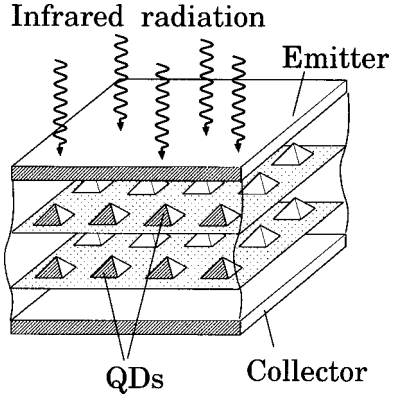

FIG. 1. Schematic view of the QDIP structure.

[a]Electronic mail: v-ryzhii@u-aizu.ac.jp

ture, and limitations imposed on the QD filling by the Pauli principle, the existence of the passes for mobile electrons between QDs, the activation character of the electron capture due to the repulsive potential of charge QDs, and thermionic nature of the injection. As shown previously,[1,16,17] these features lead to a significantly lower average probability of the electron capture in QDIPs compared to that in QWIPs and to a pronounced dependence of this probability on the applied voltage. The latter effects are associated with a decrease in the capture probability with increasing average number of electrons in QDs, N. The number of electrons occupying the QDs, in turn, increases when the applied voltage increases (analogously with that in induced base hot electron transistors and QWIPs with thermionic injection).[21–23] The sensitivity of capture probability on the QD filling, naturally, results in a voltage-dependent current gain and, consequently, in a fairly steep dark current–voltage and photocurrent–voltage characteristics of QDIPs, which occur to be exponential as observed experimentally.[6,8] Thus, the QDIP responsivity can be markedly higher than the responsivity of QWIPs. However, simultaneously QDIPs exhibit larger dark current than QWIPs do. The electron charges induced in QDs in QDIPs with thermionic injection by the applied voltage affect, as shown in the following, the QDIP detectivity as well.

Indeed, as follows, in particular, from Ref. 24, the detectivity, D^*, for a thermally-limited detection can be expressed in terms of the total thermoexcitation and photoexcitation rates G^{dark} and G^{ph} from the QDIP unit area:

$$D^* = \frac{G^{ph}}{2\hbar\Omega I\sqrt{G^{dark}}}, \tag{1}$$

where Ω and I are the photon frequency and flux, respectively, and $\hbar$ is the Planck constant. In the QDs under consideration (with the transverse size much smaller than the lateral sizes, a large number of bound states, and widely distributed energy levels), electrons form a two-dimensional electron gas. Taking this into account, the rate of thermoexcitation can be presented in the form:

$$G^{dark} = g\Sigma_{QD}K\exp\left(-\frac{\epsilon_I}{k_BT}\right)\left[\exp\left(\frac{\pi\hbar^2 N}{mk_BTa^2}\right)-1\right] \simeq g\Sigma_{QD}K\exp\left[\frac{(\pi\hbar^2/ma^2)N-\epsilon_I}{k_BT}\right]. \tag{2}$$

The rate of photoexcitation is given by

$$G^{ph} = \sigma I\Sigma_{QD}KN. \tag{3}$$

Here, g is the pre-exponential factor, a is the QD lateral size (so that the QD lateral area is equal to a^2), Σ_{QD} is the sheet density of QDs in each QD array, K is the number of the QD arrays in the QDIP, ϵ_I is the ionization energy of the ground state in QDs, T is the temperature, σ is the photoescape cross section, k_B is Boltzmann constants, and m is the effective mass of electrons in QDs.

Using Eqs. (1)–(3), we arrive at the following formula for the QDIP detectivity:

$$D^* = \frac{\sigma}{2\hbar\Omega}\sqrt{\frac{K\Sigma_{QD}}{g}}N\exp\left[\frac{\epsilon_I-(\pi\hbar^2/ma^2)N}{2k_BT}\right]. \tag{4}$$

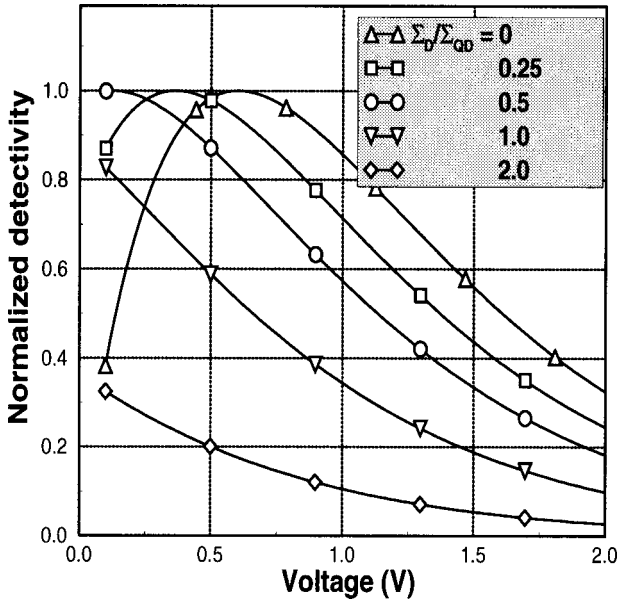

FIG. 2. Normalized detectivity versus applied voltage for QDIPs with $K=20$, $L=30$ nm, $a=15$ nm, and different donor densities at $T=80$ K.

In the voltage range $k_BT \ll eV < e(V_{QD}-V_D)$ (in which QDs are not totally filled), one can obtain:[14,15]

$$N = N_{QD}\frac{(V+V_D)}{V_{QD}}. \tag{5}$$

Here, N_{QD} is the maximum number of electrons which can be accepted by each QD, V is the applied voltage, $V_D = 2\pi eK(K+1)\Sigma_D L/æ$ and $V_{QD} = 2\pi eK(K+1)\Sigma_{QD}LN_{QD}/æ$ are the characteristic voltages, where e is the electron charge, æ is the dielectric constant, L is the spacing between the QD arrays, and Σ_D is the donor sheet density per QD array.

Substituting N from Eq. (5) into Eq. (4), we obtain

$$D^* = \frac{\sigma}{2\hbar\Omega}\sqrt{\frac{K\Sigma_{QD}}{g}}\frac{N_{QD}(V+V_D)}{V_{QD}} \times\exp\left[\frac{\epsilon_I-\left(\frac{\pi\hbar^2 N_{QD}}{ma^2}\right)\frac{(V+V_D)}{V_{QD}}}{2k_BT}\right]. \tag{6}$$

Figure 2 shows the dependence of the normalized detectivity on the applied voltage for QDIPs with different doping levels and fixed density of QDs at $T=80$ K calculated using Eq. (6). It is assumed that $K=20$, $L=30$ nm, $a=15$ nm, $\Sigma_{QD}=10^{10}\,cm^{-2}$, $æ=12$, and $m=4\times10^{-29}$ g.

Using Eqs. (5) and (6), one can find that the detectivity is maximized when $N=(2ma^2k_BT/\pi\hbar^2)$ with $N<N_{QD}$. The condition of the maximum detectivity is equivalent to

$$\frac{æV}{2\pi eK(K+1)L}+\Sigma_D=\left(\frac{2mk_BTa^2}{\pi\hbar^2}\right)\Sigma_{QD}. \tag{7}$$

This condition can be satisfied at a certain voltage only if the doping level is sufficiently low:

$$\Sigma_D<\left(\frac{2mk_BTa^2}{\pi\hbar^2}\right)\Sigma_{QD}. \tag{8}$$

For QDIPs with the same parameters as those used for Fig. 2, inequality (8) yields $\Sigma_D/\Sigma_{QD} < 0.3-0.6$.

When Σ_D and/or V are chosen in such a way that condition (7) is met, assuming that $\hbar\Omega = \epsilon_I$, for the maximum of the QDIP detectivity one obtains:

$$\max D^* = \frac{\sigma}{2\hbar\Omega}\sqrt{\frac{K\Sigma_{QD}}{g}}\left(\frac{2ma^2k_BT}{\pi\hbar^2}\right)\exp\left(\frac{\hbar\Omega}{2k_BT}-1\right). \tag{9}$$

In the case of normal incidence of infrared radiation, the photoescape cross section is a function of the QD lateral size. This function, $\sigma = \sigma(a)$, decreases with increasing a. One can assume that the pre-exponential factor in Eq. (2) is $g_{QD} \propto a^2$. Thus, from Eq. (9), one can obtain $\max D^* \propto \sigma(a)\sqrt{\Sigma_{QD}a^2}$. This relationship indicates that the increase in the QDIP detectivity can be achieved by decreasing of QD sizes with simultaneous enhancement of the QD density. At very high doping levels when $\Sigma_D \geqslant N_{QD}\Sigma_{QD}$, all QDs are totally filled at any voltages. In this case, the rate of thermoexcitation becomes very high[16] leading to a very low detectivity.

Using Eqs. (9) for the maximum value of the QDIP detectivity and the pertinent expression for the QWIP detectivity (determined as in Ref. 25), one can arrive at the following estimate of the ratio of the detectivities: $\max D^*/\max D^*_{QW} \simeq (\sigma/\sigma_{QW})\sqrt{\Sigma_{QD}a^2}$, where σ_{QW} is the cross section of the electron photoescape from the QW (corresponding to a proper polarization of incident radiation). All fabricated and measured QDIPs have rather low QD densities. Hence, when $\sigma \simeq \sigma_{QW}$, the ratio of detectivities is small even if QDIPs are doped optimally. Thus, QDIPs with relatively low densities of large QDs should exhibit lower detectivity than QWIPs. This conclusion—following from our model—refutes an optimistic assumption based on just qualitative reasoning.[26] Naturally, in the case of arbitrary ratio Σ_D/Σ_{QD} [for example, when inequality (8) is broken], the QDIP detectivity can be fairly low. This explains why the QDIPs under consideration are inferior to QWIPs in detectivity. One needs to stress that these calculations and conclusions refer to QDIPs with large QDs which are capable of accepting many electrons distributed over widely spread energy levels. In QDIPs with such QDs, the electron activation energy decreases near linearly with increasing sheet concentration of electrons occupying each QD layer. When $\Sigma_{QD}a^2 \ll 1$, the density of states per unit area is small as well. Hence, the drop of the activation energy when the electron concentration increases is steeper than that in QWIPs. However, in QDIPs with a high density of small QDs (which can accept, say, two electrons), in which the activation energy can be close to the QD ionization energy, the dark current can be lowered,[1] providing a high detectivity. For the ratio of the maximum of such a QDIP detectivity and the maximum detectivity of the optimized QWIP, in which the activation energy is equal to $(\epsilon_I - 2k_BT)$ (see, for example, Ref. 25), one can obtain $\max D^*/\max D^*_{QW} \simeq (\sigma/\sigma_{QW})$.

We would like to point out that the obtained results are qualitatively valid even for QDIPs with rather small QDs which can accept few electrons. In the case of such QDIPs, the exponential dependence on N in Eq. (2) should be appropriately modified to take into account the fact that the electron energy spectrum of QD is actually not continuous.

In conclusion, we have calculated the QDIP detectivity for a thermally-limited detection as a function of the structural parameters, temperature, and applied voltage and found the conditions for its maximum. We demonstrated that the QDIP detectivity is very sensitive to doping and that the detectivity maximization is feasible by a proper choice of the applied voltage only when the ratio of the donor and QD densities is sufficiently low. We have clarified why the existing QDIPs with relatively low density QD arrays of large QDs exhibit lower detectivity than QWIPs. An improvement in the QDIP detectivity can be realized by the use of QD structures with dense arrays of small QDs.

One of the authors (V.M.) was supported by ARO Grant No. 41327-EL.

[1] V. Ryzhii, Semicond. Sci. Technol. **11**, 759 (1996).
[2] J. Phillips, K. Kamath, and P. Bhattacharya, Appl. Phys. Lett. **72**, 2020 (1998).
[3] S. Kim, H. Mohseni, M. Erdtmann, M. Michel, J. Jelen, and M. Razeghi, Appl. Phys. Lett. **73**, 963 (1998).
[4] D. Pan, E. Towe, and S. Kennerly, Appl. Phys. Lett. **73**, 1937 (1998).
[5] S. Maimon, E. Finkman, G. Bahir, S. E. Schacham, J. M. Garcia, and P. M. Petroff, Appl. Phys. Lett. **73**, 2003 (1998).
[6] S. J. Xu, S. J. Chua, T. Mei, X. C. Wang, X. H. Zhang, H. G. Karunasiri, W. J. Fan, C. H. Wang, J. Jiang, S. Wang, and X. G. Xie, Appl. Phys. Lett. **73**, 3153 (1998).
[7] N. Horiguchi, T. Futatsugi, Y. Nakata, N. Yokoyama, T. Mankad, and P. M. Petroff, Jpn. J. Appl. Phys., Part 1 **38**, 2559 (1999).
[8] J. Phillips, P. Bhattacharya, S. W. Kennerly, D. W. Beekman, and M. Dutta, IEEE J. Quantum Electron. **35**, 936 (1999).
[9] D. Pan, E. Towe, and S. Kennerly, Appl. Phys. Lett. **75**, 2719 (1999).
[10] L. Chu, A. Zrenner, G. Böhm, and G. Abstreiter, Appl. Phys. Lett. **75**, 3599 (1999).
[11] E. Towe and D. Pan, IEEE J. Sel. Top. Quantum Electron. **6**, 408 (2000).
[12] S.-W. Lee, K. Hirakawa, and Y. Shimada, Appl. Phys. Lett. **75**, 1428 (1999).
[13] T. Cho, J.-W. Kim, J.-E. Oh, J.-W. Choe, and S. Hong, Jpn. J. Appl. Phys., Part 1 **38**, 2442 (1999).
[14] N. Rappaport, E. Finkman, T. Brunhes, P. Boucaud, S. Sauvage, N. Yam, V. Le Thanh, and D. Boucher, Appl. Phys. Lett. **77**, 3224 (2000).
[15] H. C. Liu, M. Gao, J. McCaffrey, Z. R. Wasilewski, and S. Fafard, Appl. Phys. Lett. **78**, 79 (2001).
[16] V. Ryzhii, V. Pipa, I. Khmyrova, V. Mitin, and M. Willander, Jpn. J. Appl. Phys., Part 2 **39**, L1283 (2000).
[17] V. Ryzhii, Jpn. J. Appl. Phys., Part 2 **40**, L148 (2001).
[18] Y. Toda, O. Moriwaki, M. Nishioka, and Y. Arakawa, Phys. Rev. Lett. **82**, 4114 (1999).
[19] R. Fereira and G. Bastard, Appl. Phys. Lett. **74**, 2818 (1999).
[20] J. Feldmann, S. T. Cudiff, M. Arzberger, G. Böhm, and G. Abstreiter, Appl. Phys. Lett. **89**, 1180 (2001).
[21] S. Luryi, IEEE Electron Device Lett. **6**, 178 (1985).
[22] V. Ryzhii and M. Ershov, J. Appl. Phys. **78**, 1214 (1995).
[23] A. G. U. Perera, S. G. Matsik, H. C. Liu, M. Gao, M. Buchanan, W. J. Schaff, and W. Yeo, Appl. Phys. Lett. **77**, 741 (2000).
[24] I. Grave and A. Yariv, *Intersubband Transitions in Quantum Wells*, edited by E. Rosencher, B. Vinter, and B. Levine (Plenum, New York, 1992) p. 15.
[25] M. J. Kane, S. Millidge, M. T. Emeny, D. Lee, D. R. P. Guy, and C. R. Whitehouse, *Intersubband Transitions in Quantum Wells*, edited by E. Rosencher, B. Vinter, and B. Levine (Plenum, New York, 1992) p. 31.
[26] E. Finkman, S. Maimon, V. Immer, G. Bahir, S. E. Schacham, F. Fossard, F. H. Julien, J. Brault, and M. Gendry, Phys. Rev. B **63**, 045323 (2001).